

Fluctuation of the Top Location and Avalanches in the Formation Process of a Sandpile

Chiyori URABE*

Graduate School of Science, Kyoto University, Kyoto 606-8501

We investigate the formation processes of a sandpile using numerical simulation. We find a new relation between the fluctuation of the motion of the top and the surface state of a sandpile. The top moves frequently as particles are fed one by one every time interval T . The time series of the top location has the power spectrum which obeys a power law, $S(f) \sim f^\alpha$, and its exponent α depends on T and the system size w . The surface state is characterized by two time scales; the lifetime of an avalanche, T_a , and the time required to cause an avalanche, T_s . The surface state is fluid-like when $T_a \sim T_s$, and it is solid-like when $T_a \ll T_s$. Our numerical results show that α is a function of T_s/T_a .

KEYWORDS: sandpile, fluctuation, the top location, power spectrum, power law, avalanche, fluid state, solid state, granular system, numerical simulation

1. Introduction

It is known that the state of a granular system changes between solid-like state and fluid-like state.¹⁻⁶⁾ A sandpile in the formation process is a typical system in which the both states appear. Its state is solid-like when the feed rate of particles to the sandpile is sufficiently small, and the stress in the sandpile localizes in certain particles.⁷⁻¹⁰⁾ Contrastingly, the surface of the sandpile is in fluid-like state when the feed rate is large because avalanches occur frequently, and it is reported that the magnitude distribution of avalanches depends on the grain shape and the system size.¹¹⁻¹³⁾ In particular, the surface state varies locally and with time, and it is controlled by the feed rate. Elucidation of the transition of the state is one of interesting problems in granular systems.

In the previous paper,¹⁴⁾ we studied numerically the formation process of a two-dimensional sandpile. We found that the power spectrum of the time series of the top location, $S(f)$, obeys generically a power law, $S(f) \sim f^\alpha$, and that the exponent α depends on the feed rate. We defined the left(right) mode as the state which avalanches occur mainly on the left(right) slope of the sandpile. In the case where the feed rate is large, if we introduce a two-valued function K which takes -1 when the left mode appears and 1 when the right mode does, the power spectrum of the time series of K obeys a power law, and its exponent is equal to α .

*E-mail adress: chiyori@scphys.kyoto-u.ac.jp

In this paper, we investigate the fluctuation of the top location and avalanches in two-dimensional and three-dimensional sandpiles in more detail. Avalanches occur on the surface of the sandpile, and the surface state is characterized by two time scales; the lifetime of an avalanche, T_a , and the time required to cause an avalanche, T_s . We find that the surface state which changes between fluid-like state and solid-like state and α depend on T_s/T_a for a two-dimensional sandpile. We redefine the left(right) mode as the state that almost avalanches in a time interval occur on the left(right) slope and observe the continuation of the left or right mode for sufficiently long time. We find that the reason of the continuation is that the memory of the mode is stored in the shape of the sandpile. In addition, also for a three-dimensional sandpile, the power spectrum of the time series of the top location obeys a power law with the exponent which depends on the feed rate.

This paper is organized as follows. In the next section, we describe the simulation method and the setup of the system. In Sec.3, for the two-dimensional sandpile, it is shown that the power spectrum of the top location obeys a power law with the exponent α which depends on T and w . In Sec.4, we consider avalanches in the two-dimensional sandpile. In Sec.5, the relations among T_a, T_s and α are discussed. In Sec.6, we present the results for the three-dimensional sandpile. Sec.7 is devoted to discussion and summary.

2. Discrete Element Method

We numerically simulate the motion of particles using the discrete element method (DEM).¹⁵⁾ Particles are circular in a two-dimensional system or spherical in a three-dimensional system with the radii uniformly distributed in the range $[0.8d, d]$. The force of gravity acts on every particle, and elastic force, viscous force and coulomb friction affect each pair of particles in contact. Let m_i , I_i and r_i denote the weight, the moment of inertia and the radius of the i th particle, respectively. The center of mass, \mathbf{x}_i , and the angular velocity ω_i of the i th particle obey the following equations of motion.

$$m_i \ddot{\mathbf{x}}_i = \sum_j \Theta(X_{ij})(F_n^{ij} \mathbf{n}_{ij} + \mathbf{F}_t^{ij}) + m_i \mathbf{g}, \quad (1)$$

$$I_i \dot{\omega}_i = r_i \sum_j \Theta(X_{ij}) \mathbf{n}_{ij} \times \mathbf{F}_t^{ij}, \quad (2)$$

where Θ is the Heaviside function, and \mathbf{n}_{ij} and X_{ij} are defined as

$$\mathbf{n}_{ij} = (\mathbf{x}_j - \mathbf{x}_i) / |\mathbf{x}_j - \mathbf{x}_i|,$$

and

$$X_{ij} = r_i + r_j - |\mathbf{x}_i - \mathbf{x}_j|,$$

respectively. The normal contact force $F_n^{ij} \mathbf{n}_{ij}$ and the tangential contact force \mathbf{F}_t^{ij} are calculated as follows. We define F_n^{ij} as

$$F_n^{ij} = \tilde{F}_n^{ij} \Theta(-\tilde{F}_n^{ij}), \quad (3)$$

where

$$\tilde{F}_n^{ij} = -k_n X_{ij} - \eta_n \mathbf{n}_{ij} \cdot (\dot{\mathbf{x}}_i - \dot{\mathbf{x}}_j), \quad (4)$$

commonly in the two and three dimensional systems. The function $\Theta(-\tilde{F}_n^{ij})$ means that particles are cohesionless. Parameters k_n and η_n represent the spring constant and the viscous coefficient in the normal direction.

We employ different definition of \mathbf{F}_t^{ij} in the two and three dimensional systems. In the two-dimensional system, \mathbf{F}_t^{ij} is defined as in the previous paper,¹⁴⁾

$$\mathbf{F}_t^{ij} = k_t u_t^{ij} \mathbf{t}_{ij}, \quad (5)$$

where \mathbf{t}_{ij} is the tangential vector, and k_t is the spring constant in the tangential direction. Displacement u_t^{ij} is given by the integration of the following equation under the condition that the i th and j th particles are in contact, that is when $|\mathbf{x}_j - \mathbf{x}_i| \leq r_j + r_i$.

$$\dot{u}_t^{ij} = -\left((\dot{\mathbf{x}}_i - \dot{\mathbf{x}}_j) \cdot \mathbf{t}_{ij} + r_i \omega_i + r_j \omega_j \right) \Theta(\mu |F_n^{ij}| - |F_t^{ij}|), \quad (6)$$

where μ is the friction coefficient, and u_t^{ij} is zero when $|\mathbf{x}_j - \mathbf{x}_i| > r_j + r_i$. In the three-dimensional system, \mathbf{F}_t^{ij} is defined as follows.

$$\mathbf{F}_t^{ij} = \begin{cases} \tilde{\mathbf{F}}_t^{ij} & \text{if } |\tilde{\mathbf{F}}_t^{ij}| < \mu |F_n^{ij}|, \\ \mu F_n^{ij} \mathbf{e}_t^{ij} & \text{otherwise,} \end{cases} \quad (7)$$

where

$$\tilde{\mathbf{F}}_t^{ij} = -k_t \Psi - \eta_t (\mathbf{n}_{ij} \times (\dot{\mathbf{x}}_j - \dot{\mathbf{x}}_i) + r_i \omega_i + r_j \omega_j) \times \mathbf{n}_{ij},$$

$$\Psi = \sum_{l=1}^2 \mathbf{t}_l \int_{t_0}^t dt' \tilde{\Psi}(t') \cdot \mathbf{t}_l(t'),$$

$$\tilde{\Psi}(t') = (r_i \omega_i + r_j \omega_j) \times \mathbf{n}_{ij}(t') + \dot{\mathbf{x}}_j(t') - \dot{\mathbf{x}}_i(t'),$$

$$\mathbf{e}_t^{ij} = \frac{\mathbf{F}_t^{ij}}{|\mathbf{F}_t^{ij}|}.$$

Time t_0 is the time when the i th and j th particles begin to contact. Parameter η_t is the viscous coefficient in the tangential direction. The tangential vectors, \mathbf{t}_1 and \mathbf{t}_2 , are unit vectors perpendicular to \mathbf{n}_{ij} .

There are two physical differences for the tangential forces in the two and three dimensional systems. One is that viscous term is absent in the two-dimensional system, while it is present in the three-dimensional system. Although the latter describes more general cases,

Table I. Variables and Parameters

	2D	3D
m_i	$m(2r_i/d)^2$	$m(2r_i/d)^3$
I_i	$m_i r_i^2/2$	$2m_i r_i^2/5$
$k_n[mg/d]$	1.0×10^4	1.0×10^4
$\eta_n[m\sqrt{d/g}]$	1.0×10^2	1.4×10^2
$k_t[mg/d]$	2.0×10^3	2.5×10^3
$\eta_t[m\sqrt{d/g}]$	0	7.2×10
μ	0.5	0.2
w	$20d, 40d, 80d, 160d$	$30d$

we emphasize consistency with the previous work.¹⁴⁾ The other is that the tangential shear has the maximum value in the two-dimensional system, while there is no limit on the shear in the three-dimensional system. In the two-dimensional system, we assume that the shear beyond the limit does not affect because particles slip. Although these differences influence significantly dense systems with strong shear acting continuously, we infer that the influence is noncritical for our sandpile systems because the contact time is not very long.

Parameter values used in our simulation are listed in Table I, and the physical quantities are rescaled to be dimensionless where m represents the weight of a particle with radius d . The restitution constants in two and three dimensional systems are respectively about 0.3 and 0.2 with the values in Table I.

We make a sandpile on a table which has the origin of coordinates at the center. The table in the two-dimensional system is illustrated in Fig. 1 (a). It consists of an alignment of particles with diameter d on the x -axis, and its length is w . In the three-dimensional system, the table is a flat circular plate with diameter w on the xy plane as shown in Fig.1(b). It has fixed particles with diameter $0.8d$ on its fringe. The contact force between particles and the plate is calculated in the same manner as that between two particles.

We carry out simulations using a initial sandpile which is large to cover the table. The size of a sandpile is kept virtually constant because particles are eliminated if they fall from the table. For a three-dimensional initial sandpile, after we feed sufficiently many particles and make an initial sandpile, we fix the particles remained in the sandpile for a long time to reduce calculation cost. We use Adams-Bashforth method to calculate the time evolution of particles, and the time step is $\delta t = 1.0 \times 10^{-3}$.

We feed particles to the sandpile as follows. Particles are dropped one by one from above the origin every time interval T whether avalanches occur or not. The height from which particles are dropped, H , is measured from the surface in the two-dimensional sandpile, and

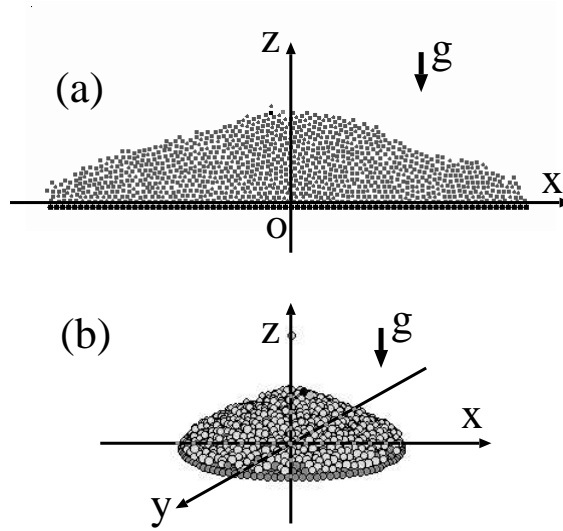


Fig. 1. The two-dimensional sandpile for $w = 80d$ (a) and (b) the three-dimensional sandpile for $w = 30d$ (b).

H is fixed to keep the collision impact given by dropped particle constant. Thus, the height from the table changes with time. In the three-dimensional sandpile, we fix the height from the table, H' , for facilitation of experiments with the same setting.

3. Fluctuation of the Top Location in the Two-Dimensional Sandpile

The top location is defined as the center of mass of the highest particle in contact with others. This quantity indicates the shape of a sandpile, and the top is moved by avalanches.

we measure the horizontal position of the top, x_{top} , in the two-dimensional sandpile and calculate the power spectrum of the time series of x_{top} for given parameter set (w, H, T) to characterize the motion of the top. For each parameter set, the power spectrum $S(f)$ is obtained through the sample average, and the average is over the power spectra of more than ten time series with the length $10^4 \sqrt{d/g}$. In the previous paper,¹⁴⁾ only for $w = 80d$, we found that $S(f)$ obeys a power law, $S(f) \sim f^\alpha$, and that the exponent α increases as T decreases, while α is independent of H .

In this paper, we look into the dependence of α on w . Exponent α is calculated by applying the least-squares method for the double logarithmic plot of $S(f)$ in the frequency range $0.0005 < f < 0.01$. Fig.2 shows that α tends to decrease with w and increases drastically as T decreases in the range $T < 10\sqrt{d/g}$ not only when $w = 80d$ but also in cases where $w = 20d$ and $40d$. For $w = 160d$, however, the range in which α changes with T is small. In Sec.5, we consider again the dependence of α on w through the relation between α and avalanches.

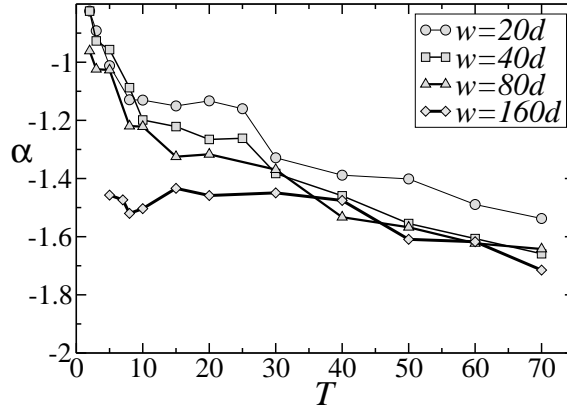


Fig. 2. Dependence of α on T and w for $H = 20d$

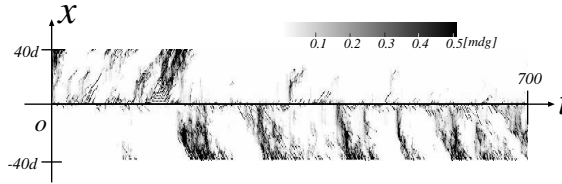


Fig. 3. The time-space plot of kinetic energy for $(w, H, T) = (80d, 20d, 2\sqrt{d/g})$.

4. Avalanches in the Two-Dimensional Sandpile

4.1 Avalanches for small T

To observe avalanches, we show the time-space plot of kinetic energy for small T in Fig.3. The gray scale represents the value of kinetic energy of particles at position x . The kinetic energy is high at $x = 0$ because particles land there. Avalanches continue for a long time on the left slope which is the lower half in Fig.3, and the duration time is sufficiently large in comparison with T .

In the previous paper,¹⁴⁾ to measure avalanches on each slope, we calculated kinetic energy of particles in the left or right half of the sandpile. The kinetic energy in each part defined as the range $x > d$ or $x < -d$ is denoted by k_l or k_r . The magnitude relation between k_l and k_r changes with time. We defined $K(t)$ as

$$K(t) = \begin{cases} 1, & \text{if } k_l(t) < k_r(t), \\ -1, & \text{otherwise,} \end{cases} \quad (8)$$

and we called the state that $K = 1$ ($K = -1$) the right(left) mode. For small T , the exponents of the power spectra of x_{top} and K are approximately equal in a low frequency range.

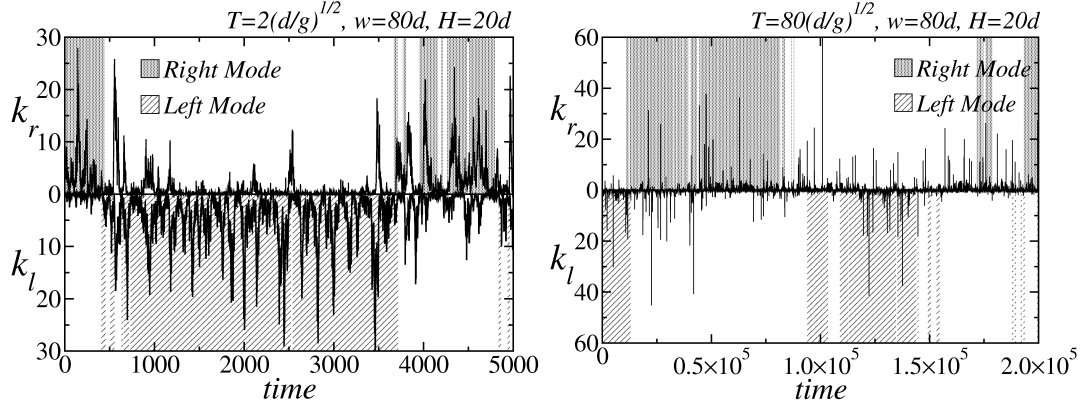


Fig. 4. The time series of k_l and k_r in the cases where $(w, H, T) = (80d, 20d, 2\sqrt{d/g})$ and $(80d, 20d, 80\sqrt{d/g})$ are plotted. The newly-defined mode is shown with $\Delta t = 50T$.

4.2 Redefinition of the mode

To investigate the mode in more detail, we redefine the mode which depend on the state of avalanches for a long time scale. Because the current definition determined by instantaneous magnitude of avalanche, it is not able to operate when avalanches occur intermittently.

We redefine the mode using K' defined as follows.

$$K'(t) = \begin{cases} 1, & \text{if } k_r(t) > k_l(t), \\ 0, & \text{if } k_r(t) = k_l(t), \\ -1, & \text{if } k_r(t) < k_l(t). \end{cases} \quad (9)$$

The term, $K' = 0$, is needed in the case where T is large. We define newly the right(left) mode as the state that the time for $K' = 1(K' = -1)$ amounts to more than $\gamma\Delta t$ in the time $[t - \Delta t/2, t + \Delta t/2]$ where $0.5 < \gamma < 1$, and Δt is a sufficiently large constant in comparison with T . In addition, we introduce the competitive mode defined as the state that the fractions of $K' = 1$ and $K' = -1$ are comparable.

In Fig.4, we show the time series of k_l and k_r and the newly-defined mode with $\gamma = 0.8$ for $T = 2\sqrt{d/g}$ and with $\gamma = 0.6$ for $T = 80\sqrt{d/g}$. Long-lived modes are observed not only for small T but also for large T .

4.3 Continuation of the mode

We infer that the mode continues because its memory is stored in either of the shape of the sandpile or the motion of particles. To determine which of them is more important factor, we carry out examinations as follows. We stop adding particles at a time and restart adding after waiting until all particles cease, and we calculate the mode before stop and after restart. If the same mode tends to appear before stop and after restart, we consider that its memory is stored in the shape because the motion of particles ceases before adding particle is restarted. Adding particles is restarted at the time when k_l and k_r decrease to a constant k^* .

Table II. In the case of L or R before stop

After\Before	L or R
Same	58%
C	40%
Contrary	2%
total	139 data

Table III. In the case of C before stop

After\Before	C
C	72%
L or R	28%
total	211 data

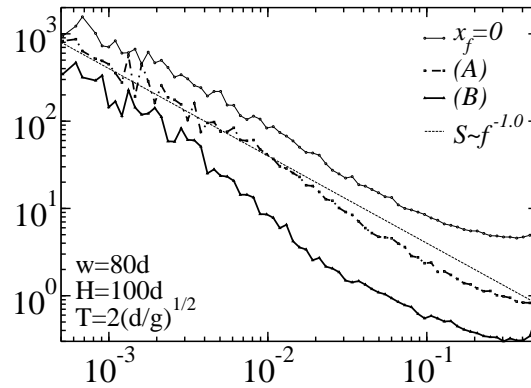


Fig. 5. The power spectrum of x_{top} for $(w, H, T) = (80d, 100d, 2\sqrt{d/g})$ in the cases (A), (B) and $x_f = 0$.

This examination is repeated randomly, and the results show that the memory is stored in the shape. TableII shows the results on the fraction of the mode after restart in the case of the left(L) or right(R) mode before stop adding, and TableIII shows that in the case of the competitive(C) mode, for $(w, H, T) = (80d, 20d, 2\sqrt{d/g})$ where $\Delta t = 50T$, $\gamma = 0.8$, and $k^* = 1.0 \times 10^{-6}mdg$. Although the competitive mode appears more frequently than the left or right mode in this criterion, the fraction that the same mode appears in TableII is higher than other modes. In addition, also in TableIII, the fraction of the same mode is significantly high.

4.4 Relation between the fluctuation of the top location and the position of adding particles

To clarify relations between the motion of the top and avalanches, we change the position of adding particles because we infer that the relations change with the position. We choose

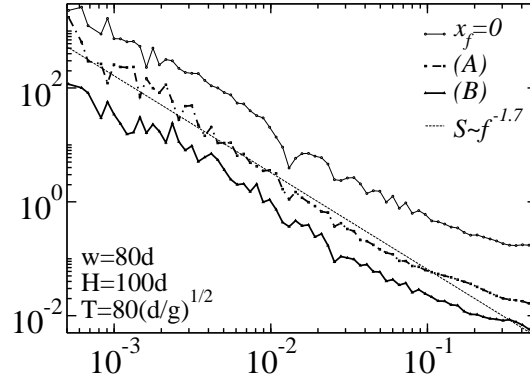


Fig. 6. The power spectrum of x_{top} for $(w, H, T) = (80d, 100d, 80\sqrt{d/g})$ in the cases (A), (B) and $x_f = 0$.

randomly the horizontal position at which particles are dropped, x_f , in a range and carry out experiments for the two cases (A) and (B); (A) is the case where particles are fed uniformly above the whole table, $-w/2 < x_f < w/2$, and (B) is the case where we omit a vicinity of the top from the range, $w_e < |x_f| < w/2$ where w_e is a constant. In both cases, we calculate the power spectrum of x_{top} for $(w, H, T) = (80d, 100d, 2\sqrt{d/g})$ and $(80d, 100d, 80\sqrt{d/g})$ and compare with that in the case $x_f = 0$.

In the cases of $x_f = 0$ and (A), the exponents of the power spectra are equal in a low frequency range. The thick dashed lines in the Fig.5 and Fig. 6 show the power spectra in the case (A). For reference, in the case $x_f = 0$, we plot the power spectra (thin solid lines) and the power functions with the exponent which is the same with that of the power spectra (thin dashed lines), respectively.

In addition, for small T , the exponent of the power spectrum depends on whether particles are fed near the top or not. The thick solid lines in Fig.5 and Fig. 6 indicate the power spectra in the case (B) where $w_e = 10d$ because $-10d < x_{top} < 10d$ in the case $x_f = 0$. Although the exponents in the cases (B) and $x_f = 0$ are almost equal for $T = 80\sqrt{d/g}$, the exponents in the case (B) is smaller than that in the case $x_f = 0$ for $T = 2\sqrt{d/g}$.

For small T , we consider that the motion of the top is different in the cases (B) and $x_f = 0$ because avalanches change with the position of adding particle. Avalanches are frequently accelerated by the impact of fed particles for small T , and we infer that the probability of the acceleration decreases with the distance between the landing position of fed particles and the top because the landing position approaches downstream of avalanches. Therefore, the motion of the top changes with the distance. Contrastingly, for large T , in both cases $x_f = 0$ and (B), the probability is low because avalanches induced by a fed particle cease before the next particle is fed, hence there is no difference in the motion of the top.

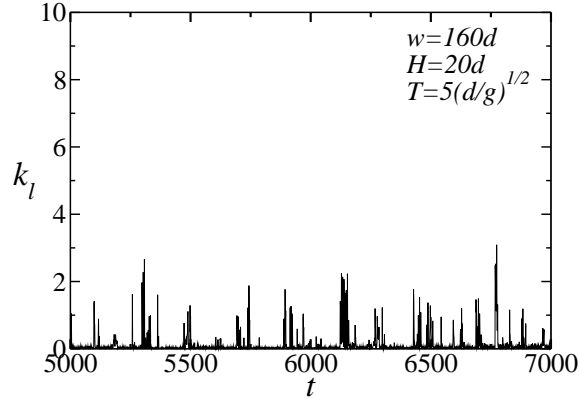


Fig. 7. The time series of k_l for $(w, H, T) = (160d, 20d, 5\sqrt{d/g})$

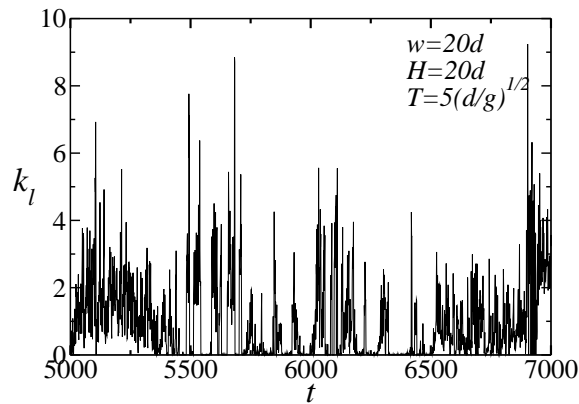


Fig. 8. The time series of k_l for $(w, H, T) = (20d, 20d, 5\sqrt{d/g})$

5. Fluid-Like State in the Surface of a Sandpile

In this section, we try to obtain a quantitative relation between the states of the surface of a sandpile and the exponent of the power spectrum of x_{top} , α . We infer that the state is characterized by some time scales for avalanches, and that the motion of the top is related to the time scales because the top is moved mainly by avalanches.

The surface state and α depend on not only T but also w . Actually, α for $(w, H, T) = (160d, 20d, 5\sqrt{d/g})$ is smaller than that for smaller w and the same T as shown in Fig.2. As shown in Fig. 7 and Fig. 8, k_l for $w = 160d$ is clearly smaller than that for $w = 20d$, and such small kinetic energy is characteristic of the solid-like state, while the state for $w = 20d$ is fluid-like.

5.1 Time scales for avalanches

The surface state is related to two time scales for avalanches. One is the time required to cause an avalanche, and the other is the lifetime of an avalanche. In the case where the former is sufficiently larger than the latter, the state is kept solid-like because the time between

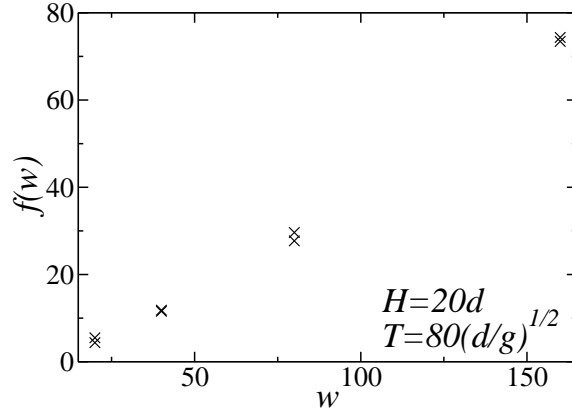


Fig. 9. We calculate $f(w)$ from the time series of N_l or N_r with the length $2.0 \times 10^6 \sqrt{d/g}$ for $(H, T) = (20d, 80\sqrt{d/g})$.

avalanches is long. Contrastingly, the state is fluid-like when these time scales are comparable.

The lifetime of an avalanche, T_a , is independent of w . Lifetime T_a is calculated as the average of the duration time in which k_l or k_r is kept larger than a constant k_a . The duration time of an avalanche is well-defined when the feed rate is small because each avalanche is plainly distinguishable. Therefore, we calculate the time scales for large T . Our numerical results with $k_a = 0.05mdg$ show that T_a is around $5.0\sqrt{d/g}$ for $w = 20d, 40d, 80d$ and $160d$ when $(H, T) = (20d, 80\sqrt{d/g})$.

The time required to cause an avalanche, T_s , depends on T and w . Time T_s is defined as the time required to accumulate sufficient amount of particles for causing an avalanche. We postulate that T_s is proportional to T , and T_s is represented as follows,

$$T_s = T f(w), \quad (10)$$

where $f(w)$ is the typical size of an avalanche and defined as the standard deviation of $N_l(t)$ or $N_r(t)$, where $N_l(t)$ and $N_r(t)$ is respectively the number of particles in the left half and right half of a sandpile at time t . The left half is defined as the part in the range $-w/2 > x > -1.5d$, and the right half is the part in the range $1.5d < x < w/2$. We find that $f(w)$ increases with w as shown in Fig9.

The results show that the fluid-like state of the surface is kept for a long time if T and w are small because T_a and T_s are comparable, and that the state is solid-like if T or w is large because $T_a \ll T_s$.

The exponent α is related to the surface state and a function of T_s/T_a . We assume that α depends on the ratio T_s/T_a and rescale the data in Fig.2 by $T^* = T_a/f(w)$. The result is shown in Fig.10. However, to judge whether α depends on only T/T^* , more elaborate simulation is needed to determine α , T_a and T_s more precisely.

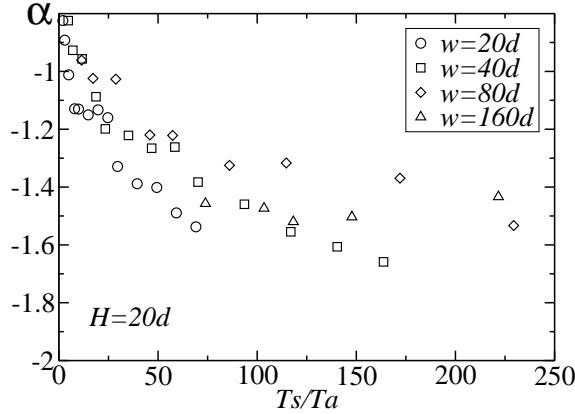


Fig. 10. The dependence of α on T_s/T_a when $H = 20d$ and $T_a = 5\sqrt{d/g}$

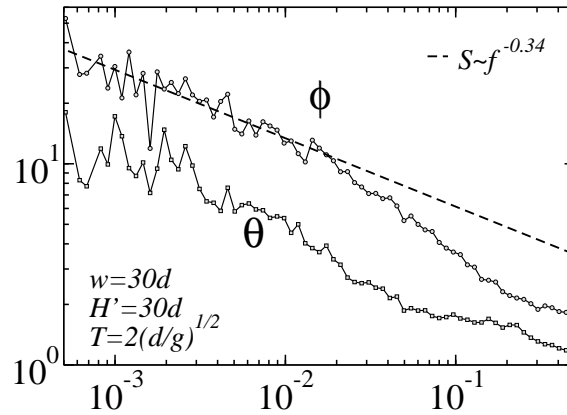


Fig. 11. Power spectra of ϕ (upper solid line) and θ (lower solid line) for $(w, H', T) = (30d, 30d, 2\sqrt{d/g})$. We move down the plot for θ in parallel to distinguish lines.

6. Fluctuation of the Top Location and Avalanches in the Three-Dimensional Sandpile

6.1 Dependence of fluctuation of the top location on T

In the three-dimensional sandpile, we measure the top location by the cylindrical coordinates and calculate the power spectrum of the time series of its azimuthal angle ϕ where $-\pi \leq \phi \leq \pi$ as in the same manner for the two-dimensional sandpile. The power spectrum obeys a power law, $S(f) \sim f^{\alpha_\phi}$, in a low frequency range as shown in Fig.11. Exponent α_ϕ is obtained by a least-square fit of the double logarithmic plot of the power spectrum in the frequency range $0.0005 < f < 0.01$. Dependence of α_ϕ on T is shown in Fig.12, which is similar to Fig.2 for α in the two-dimensional sandpile, although α_ϕ is larger than α . We consider that a reason why $\alpha_\phi < \alpha$ is because w is small in the three-dimensional systems.

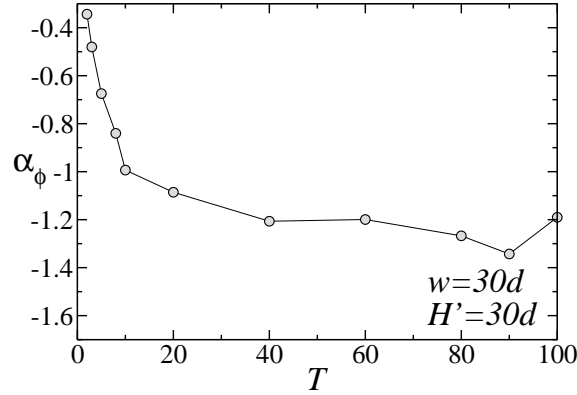


Fig. 12. Dependence of α_ϕ on T for $(w, H') = (30d, 30d)$.

6.2 Relation between the motion of the top and avalanches

We consider the direction of an avalanche projected on the horizontal plain. The direction is represented by the average of particle momentum, (\bar{p}_1, \bar{p}_2) , which is defined by the following equation,

$$\bar{p}_l = \frac{1}{N} \sum_{i=1}^N m_i v_{i,l}, \quad (l = 1, 2) \quad (11)$$

where N denotes the number of particles on the table, and $v_{i,1}$ and $v_{i,2}$ are x and y directional velocities of the i th particle, respectively. We define the direction of an avalanche as the azimuthal angle of the vector (\bar{p}_1, \bar{p}_2) , θ , where $-\pi \leq \theta \leq \pi$.

To characterize the time series of θ , we show its power spectrum in Fig.11. The power spectrum is proportional to that of ϕ in a low frequency range.

7. Discussion

In our sandpile system and granular flow in a vertical pipe, there are similar relations between the exponent of the power spectrum and the phase space volume of each particle. The exponent of the power spectrum of the top location depends on the feed rate in the sandpile, and the power spectrum of the density wave in the pipe obeys also a power law¹⁶⁻²⁶⁾ with the exponent which depends on the inflow rate to the pipe.^{20,23)} If the power spectrum S_d obeys a power law, $S_d \sim f^\beta$, the exponent β increases with the volume in the phase space where each particle able to move freely. The phase space volume is decreased by restraint conditions which are different in the sandpile and flow in the pipe. In the sandpile, the volume in kinetic momentum space increases with the feed rate. In this case, avalanches occur frequently, and the surface state becomes fluid-like. In the pipe, the volume in kinetic momentum space and position space are decreased with the inflow rate because clusters appear in the flow. Developing these investigation, for granular systems, it is anticipated that the relations between the local state, such as fluid-like or solid-like, and the power spectrum in each systems are

clarified analytically.

We have investigated relations between the fluctuation of the top location and avalanches in formation process of a sandpile using numerical simulations. The top location is moved as particles are added one by one every time interval T , and its power spectrum $S(f)$ obeys a power law, $S(f) \sim f^\alpha$, in a long time scale. We found that the exponent α decreases with T and the system size w .

In a two-dimensional sandpile, we defined the right(left) mode as the state that avalanches occur mainly on the right(left) slope of the sandpile, and we found that the duration time of the left or right mode tends to be long compared to T because the memory of the mode is stored in the shape of the sandpile. In a three-dimensional sandpile, the direction of avalanches in the horizontal plane changes with time, and the power spectra of the top and the direction have the same exponent in a low frequency range for small T .

The surface state of the sandpile and the exponent α depend on the ratio between the lifetime of an avalanche, T_a , and the time required to cause an avalanche, T_s . Our numerical results show that T_a is a constant independent of w , while T_s increases with w and T . Therefore, the state is kept fluid-like when T and w are small because $T_a \sim T_s$, and it is solid-like when w or T is large because $T_a \ll T_s$. The state relates to the exponent α , and we found that α is a function of T_s/T_a .

Acknowledgment

I appreciate helpful comments with Hisao Hayakawa, Hiroyuki Tomita, Shinji Takesue, Mitsusada Sano and So Kitsunezaki. The numerical calculations were carried out on Altix3700 BX2 at YITP in Kyoto University.

References

- 1) R. M. Nedderman: *Statics and Kinematics of Granular Materials* (Cambridge, Cambridge, 1992)
- 2) H. M. Jaeger, S. R. Nagel, and R. P. Behringer: *Rev. Mod. Phys.* **68** (1996) 1259.
- 3) L. P. Kadanoff: *Rev. Mod. Phys.* **71** (1999) 435.
- 4) J. Duran: *Sands, Powders, and Grains* (Springer, New York, 2000)
- 5) T. Pöschel and S. Luding: *Granular Gasses* (Springer, New York, 2001)
- 6) T. Pöschel and N. Brilliantov: *Granular Gas Dynamics* (Springer, New York, 2003)
- 7) J. P. Wittmer, P. Claudin, M. E. Cates, and J.-P. Bouchaud: *Nature* **382** (1996) 336.
- 8) L. Vanel, D. Howell, D. Clark, R. P. Behringer, and E. Clément: *Phys. Rev. E* **60** (1999) R5040.
- 9) J. Geng, D. Howell, E. Longhi, R. P. Behringer, G. Reydellet, L. Vanel, E. Clément, and S. Luding: *Phys. Rev. Lett.* **87** (2001) 035506.
- 10) J. Geng, E. Longhi, R. P. Behringer, and D. W. Howell: *Phys. Rev. E* **64** (2001) 060301.
- 11) V. Frette, K. Christensen, A. Målthe-Sørensen, J. Feder, T. Jøssang and P. Meakin: *Nature* **379** (1996) 49.
- 12) E. Altshuler, O. Ramos, C. Martínez, L. E. Flores, and C. Noda: *Phys. Rev. Lett.* **86** (2001) 5490.
- 13) N. Yoshioka: *Earth, Planets, and Space* **55** (2003) 283.
- 14) C. Urabe: *J. Phys. Soc. Jpn.* **74** (2005) 2475.
- 15) P. A. Cundall and O. D. L. Strack: *Géotechnique* **29** (1979) 47.
- 16) G. Peng and H. J. Herrmann: *Phys. Rev. E* **49** (1994) R1796.
- 17) G. Peng and H. J. Herrmann: *Phys. Rev. E* **51** (1995) 1745.
- 18) S. Horikawa, A. Nakahara, T. Nakayama, and M. Matsushita: *J. Phys. Soc. Jpn.* **64** (1995) 1870.
- 19) S. Horikawa, T. Isoda, T. Nakayama, A. Nakahara, and M. Matsushita: *Physica A* **233** (1996) 699.
- 20) A. Nakahara and T. Isoda: *Phys. Rev. E* **55** (1997) 4264.
- 21) O. Moriyama, N. Kuroiwa, M. Matsushita, and H. Hayakawa: *Phys. Rev. Lett.* **80** (1998) 2833.
- 22) O. Moriyama, N. Kuroiwa, T. Isoda, T. Arai, S. Tateda, Y. Yamazaki, and M. Matsushita: in *TRAFFIC AND GRANULAR FLOW '01*, ed. M. Fukui, Y. Sugiyama, M. Schreckenberg, and D. E. Wolf (Springer, New York, 2003) p.437.
- 23) Y. Yamazaki, S. Tateda, A. Awazu, T. Arai, O. Moriyama, and M. Matsushita: *J. Phys. Soc. Jpn.* **71** (2002) 2859.
- 24) O. Moriyama, N. Kuroiwa, S. Tateda, T. Arai, A. Awazu, Y. Yamazaki, and M. Matsushita: *Prog. Theor. Phys. Supp.* **150** (2003) 136.
- 25) H. Hayakawa and K. Nakanishi: *Prog. Theor. Phys. Supp.* **130** (1998) 57.
- 26) H. Hayakawa: *Phys. Rev. E* **72** (2005) 031102.